Detectors for Discrete-Time Signals in Non-Gaussian Noise

JAMES H. MILLER, STUDENT MEMBER, IEEE, AND JOHN B. THOMAS, FELLOW, IEEE

Abstract—**The structure and performance of a class of nonlinear detectors for discrete-time signals in additive white noise are investigated. The detectors considered consist of a zero-memory nonlinearity (ZNL) followed by a linear filter whose output is compared with a threshold. That this class of detectors is a reasonable one to study is apparent from the fact that both the Neyman–Pearson optimum and the locally optimum (i.e., weak-signal optimum) detectors for statistically independent noise samples can be put into this form.**

The measure of detector performance used is the asymptotic relative efficiency (ARE) of the nonlinear detector under study with respect to a linear detector appropriate for the same detection problem. A general expression for this ARE is given along with the result that the nonlinearity maximizing this expression is any linear function of the nonlinearity in the appropriate constant-signal locally optimum detector.

To illustrate the structure and performance of these nonlinear detectors for a wide range of non-Gaussian noise distributions, three general classes of symmetric, unimodal, univariate probability density functions are introduced that are generalizations of the Gaussian, Cauchy, and beta distributions.

I. Introduction

A CONSIDERABLE body of knowledge exists on the use of statistical decision theory to test for the presence or absence of a known signal in additive noise. However, in most of this work, Gaussian noise is assumed eventually since other assumptions usually lead to mathematical difficulties. In this paper we consider a class of detectors for signals in additive noise that is specifically not assumed to be Gaussian.

An intuitively reasonable detector structure for a known discrete-time signal in additive white[1] noise is a zero-memory nonlinearity (ZNL) followed by a linear filter whose output is then compared to some threshold. That this basic structure deserves further investigation is apparent from examining the structures of the Neyman–Pearson optimum and locally (weak-signal) optimum detectors for a given signal in additive white noise, both of which have the postulated form of a ZNL, which is trivial for Gaussian noise, followed by a linear filter.

Fig. 1 gives the most general model of the detectors to be considered in this paper. In this figure, v_{ij} is a sequence of inputs to the detector. The ZNL denoted by $g_i(\cdot)$ may be time varying, as indicated by the subscript i, although most of the detectors considered here have a fixed nonlinearity $g(\cdot)$. The system $h(\cdot)$ is a discrete-time causal linear filter having a finite-duration impulse response $\{h(i): i = 1,2,\cdots,M\}$. The input signal may be either constant or time varying, and up to N independent copies of the received signal may be available (from different diversity channels, etc.). (In weak-signal situations, a large number of copies N may be needed to give satisfactory system performance.) The resulting N outputs of the filter $h(\cdot)$ are summed, and the output from the summer is compared to a fixed threshold T chosen to give the desired false-alarm probability.

Manuscript received June 16, 1971; revised September 3, 1971. This work was supported by NSF Grants GK-1439 and GK-24187 and by the U.S. Army Research Office under Contract DAHCOH-69-0012.

The authors are with the Department of Electrical Engineering, Princeton University, Princeton, N.J. 08540.

[1] By white noise, we shall mean noise in which distinct samples are statistically independent.

II. Constant Signal Case

A. Optimum and Locally Optimum Detectors

Consider the following hypothesis-testing problem representing the detection of a constant signal in additive white noise:

$$H_0^{(1)}: v_i = n_i$$
$$H_1^{(1)}: v_i = \theta + n_i, \qquad i = 1,2,\cdots,N. \tag{1}$$

For convenience, the signal θ will always be assumed positive. The noises $\{n_i: i = 1,2,\cdots,N\}$ are assumed to be a set of mutually statistically independent, identically distributed, real-valued random variables with a common pdf $f_n(x)$. The variance, if it exists, of a single noise sample n_i is denoted by σ_n^2.

From the Neyman–Pearson lemma [1, p. 201], the optimum test for $H_0^{(1)}$ versus $H_1^{(1)}$ in the sense of maximizing the detection probability for a fixed false-alarm probability compares the likelihood ratio

$$\Lambda(v) = f_1(v)/f_0(v) \tag{2}$$

with some threshold T_1 chosen to achieve the desired probability of false alarm. Here $f_i(v)$ is the pdf of the observation vector $v = [v_1,v_2,\cdots,v_N]$ under hypothesis $H_i^{(1)}$. Hypothesis $H_0^{(1)}$ or $H_1^{(1)}$ is chosen according to the rule

$$\Lambda(v) \begin{cases} > T_1 \Rightarrow H_1^{(1)} \\ < T_1 \Rightarrow H_0^{(1)}. \end{cases}$$

Because of the statistical independence of the noise, the pdf's of the observation vectors under the hypothesis and alternative are, respectively,

$$f_0(v) = \prod_{i=1}^{N} f_n(v_i) \tag{3a}$$

and

$$f_1(v) = \prod_{i=1}^{N} f_n(v_i - \theta). \tag{3b}$$

From (2) and (3), we obtain the optimum test for $H_0^{(1)}$ versus $H_1^{(1)}$:

$$t_{\text{opt}} = \sum_{i=1}^{N} g_{\text{opt}}(v_i) \begin{cases} > T_1 \Rightarrow H_1^{(1)} \\ < T_1 \Rightarrow H_0^{(1)} \end{cases} \tag{4}$$

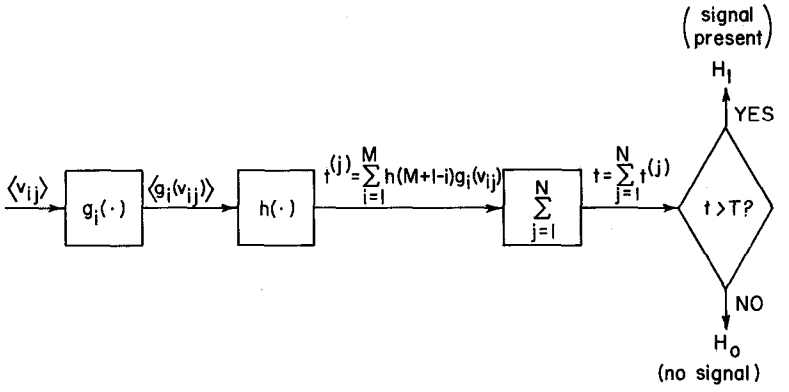

Fig. 1. General detector structure.

where the nonlinearity $g_{opt}(x)$ is defined by

$$g_{opt}(x) = \ln [f_n(x - \theta)/f_n(x)]. \tag{5}$$

This test has the structure shown in Fig. 2 with $g(\cdot)$ the $g_{opt}(\cdot)$ of (5). Note that the structure of Fig. 2 is merely a special case of that in Fig. 1.

Rather than maximizing the detection probability for a fixed false-alarm probability, the locally optimum detector for $H_0^{(1)}$ versus $H_1^{(1)}$ maximizes the slope of the power function at the origin while keeping a fixed false-alarm probability. From this requirement it can be shown [1, pp. 235–236] that the locally optimum test is

$$\Lambda'(v) \triangleq [f_0(v)]^{-1} \frac{\partial f_1(v,\theta)}{\partial \theta}\bigg|_{\theta=0} \begin{cases} > T_2 \Rightarrow H_1^{(1)} \\ < T_2 \Rightarrow H_0^{(1)}. \end{cases} \tag{6}$$

Using asymptotic relative efficiency, Capon [2] showed that, as signal strength approaches zero, the optimum and locally optimum detectors have equivalent performance. For the hypothesis-testing problem of (1), with observation pdf's given by (3a) and (3b), the locally optimum detector has the form

$$t_{lo} = \sum_{i=1}^{N} g_{lo}(v_i) \begin{cases} > T_2 \Rightarrow H_1^{(1)} \\ < T_2 \Rightarrow H_0^{(1)} \end{cases} \tag{7}$$

where the locally optimum nonlinearity $g_{lo}(x)$ is defined by

$$g_{lo}(x) \triangleq -f_n'(x)/f_n(x) = \frac{\partial}{\partial \theta} \ln f_n(x - \theta)\bigg|_{\theta=0} \tag{8}$$

It is clear that the locally optimum detector of (7) also has the structure of Fig. 2. Solving the first-order differential equation (8) gives

$$f_n(x) = K \exp \left\{ \int_0^x g(y)\, dy \right\} \tag{9}$$

as the noise pdf for which a given ZNL $g(x)$ is locally optimum.

Although the result of (9) is in itself perhaps only of academic interest, it does allow one to derive the relation between the optimum and locally optimum nonlinearities. By substituting (9) into (5), one obtains

$$g_{opt}(x) = \int_{x-\theta}^{x} g_{lo}(y)\, dy. \tag{10}$$

From this relationship it is clear that if θ is small enough

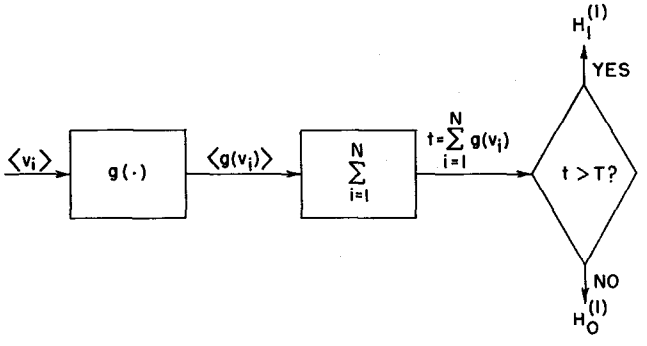

Fig. 2. Detector structure for constant signals.

and if $g_{lo}(y)$ is continuous, of one sign, and nearly constant in the interval $x - \theta \le y \le x$, then the value of the optimum nonlinearity $g_{opt}(x)$ is approximately a constant multiple of $g_{lo}(x)$, that is,

$$g_{opt}(x) \approx \theta g_{lo}(x). \tag{11}$$

From this discussion, it is easy to show certain properties that the ZNLs $g_{opt}(x)$ and $g_{lo}(x)$ must have if they are to correspond to noise pdf's of continuous-valued random variables that are symmetric and unimodal in the weak sense that if

$$|x_2| > |x_1|, \qquad \text{then } f_n(x_2) \le f_n(x_1). \tag{12}$$

From (9) any such locally optimum nonlinearity $g_{lo}(x)$ must be odd symmetric about $x = 0$ so that

$$g_{lo}(-x) = -g_{lo}(x), \qquad \text{for all } x \tag{13}$$

and be nonnegative for positive x and nonpositive for negative x. The following four properties of the Neyman–Pearson optimum nonlinearity $g_{opt}(x)$ for a positive signal θ and a symmetric unimodal noise pdf $f_n(x)$ can be derived easily from (10) and (13):

$$g_{opt}(\theta/2) = 0 \tag{14a}$$

$g_{opt}(x)$ is a strictly increasing function of x,

$$0 < x < \theta \tag{14b}$$

$$g_{opt}[(\theta/2) - x] = -g_{opt}[(\theta/2) + x] \text{ for all } x \tag{14c}$$

$$g_{opt}(x) \begin{cases} \ge 0, & x > \theta/2 \\ \le 0, & x < \theta/2. \end{cases} \tag{14d}$$

From the sets of properties in (13) and (14), it is clear

that the optimum and locally optimum nonlinearities $g_{opt}(x)$ and $g_{lo}(x)$ can differ considerably for x in the interval $[0,\theta]$. However, for $x < 0$ and $x > \theta$, the two ZNLs will be quite similar qualitatively (except for a constant of proportionality θ) if the conditions for the approximation of (11) to (10) are valid. The graphs in Section IV of corresponding optimum and locally optimum nonlinearities for specific noise densities should further clarify this discussion.

B. Comparing the Nonlinear Detector of Fig. 2 to a Linear Detector Using ARE

For the problem of testing $H_0^{(1)}$ versus $H_1^{(1)}$, it was shown in the previous section that both optimum and locally optimum detectors can be designed by using the structure of Fig. 2. This structure, with $g(\cdot)$ some appropriately chosen nonlinearity, is also suitable as a suboptimum detector for the problem. Henceforth, for convenience, a detector having the structure of Fig. 2 will be called a *constant-signal nonlinear detector.*

A convenient measure of performance for such detectors is their asymptotic relative efficiency (ARE) with respect to some reference detector [2]. If $N_i(\alpha,\beta,\theta)$ denotes the number of samples detector D_i requires to achieve a false-alarm probability α and detection probability at least equal to β with signal strength θ, the asymptotic relative efficiency of a detector D_2 with respect to a reference detector D_1 is[2]

$$\mathrm{ARE}_{2,1} = \lim_{\substack{\theta\to 0\\ N_1\to\infty\\ N_2\to\infty}} N_1(\alpha,\beta,\theta)/N_2(\alpha,\beta,\theta). \tag{15}$$

A convenient choice for the reference detector is the *linear detector* D_{ld}, which results when we place $g(x) = x$ in Fig. 2. If the noise is Gaussian, both the optimum and the locally optimum detectors are equivalent to D_{ld}. The expression for the ARE of the constant-signal nonlinear detector D_{nd} with respect to the linear detector D_{ld} is[3]

$$\mathrm{ARE}_{nd,ld} = \frac{\sigma_n^2\left[\int_{-\infty}^{\infty} g'(x)f_n(x)\,dx\right]^2}{\int_{-\infty}^{\infty} g^2(x)f_n(x)\,dx - \left[\int_{-\infty}^{\infty} g(x)f_n(x)\,dx\right]^2}. \tag{16}$$

This expression is used to evaluate the performance of optimum and suboptimum detectors for various noise pdf's in Section IV.

C. The Nonlinearity $g(x)$ That Maximizes $\mathrm{ARE}_{nd,ld}$

For a fixed noise pdf $f_n(x)$, the larger the value of $\mathrm{ARE}_{nd,ld}$, the better suited (asymptotically) is the corresponding nonlinear detector for detecting a constant signal in that particular noise. For the class of continuous, once differentiable noise pdf's, it can be shown[4] that $\mathrm{ARE}_{nd,ld}$ attains an extremum (actually, a maximum) when the nonlinearity $g(x)$ is chosen as

$$\hat{g}(x) = ag_{lo}(x) + b, \qquad a \neq 0. \tag{17}$$

This $\hat{g}(x)$ maximizes $\mathrm{ARE}_{nd,ld}$ provided that the noise density $f_n(x)$ satisfies the following two conditions:

$$0 < \sigma_n^2 = \mathrm{var}\,(x) < \infty$$

$$0 < \int_{-\infty}^{\infty} [f_n'(x)]^2[f_n(x)]^{-1}\,dx < \infty. \tag{18}$$

Furthermore, the maximum value of $\mathrm{ARE}_{nd,ld}$, denoted by ρ, is

$$\rho \triangleq \max_{g(x)} \mathrm{ARE}_{nd,ld} = \sigma_n^2 \int_{-\infty}^{\infty} [f_n'(x)]^2[f_n(x)]^{-1}\,dx. \tag{19}$$

It should be noted that the second condition in (18) is exactly that required by Capon [2] to ensure that the test statistic t_{lo} of the locally optimum detector of (7) is asymptotically normal and thus that the use of ARE is justifiable. Moreover, the fact that $\mathrm{ARE}_{nd,ld}$ will achieve an extremum if the nonlinearity $g(x)$ is chosen to be the locally optimum nonlinearity $g_{lo}(x)$, should not be surprising since both asymptotic relative efficiency and the locally optimum detector are small-signal concepts.

III. Time-Varying Signal Case

A. Optimum and Locally Optimum Detectors

When the signal is time varying instead of constant, the hypothesis testing problem of (1) may be replaced by

$$H_0^{(2)}: v_{ij} = n_{ij}$$

$$H_1^{(2)}: v_{ij} = \theta s_i + n_{ij}, \qquad i = 1,2,\cdots,M;\quad j = 1,2,\cdots,N \tag{20}$$

where the double subscripts are used to reflect the multiple-channel nature of the problem. The signal $\theta[s_1,s_2,\cdots,s_M]$ is of finite duration M. The second subscript j indexes the N different channels over which the time-varying signal is available to the receiver. All the noises n_{ij} both within one channel and between different channels are assumed to be statistically independent.

The pdf of the (multiple channel) observation vector $\boldsymbol{V}$, where

$$\boldsymbol{V} \triangleq [v_{11},\cdots,v_{M1},v_{12},\cdots,v_{M2},\cdots,v_{1N},\cdots,v_{MN}]$$

under the hypothesis $H_0^{(2)}$ is thus

$$f_0(\boldsymbol{V}) = \prod_{j=1}^{N}\prod_{i=1}^{M} f_n(v_{ij}) \tag{21a}$$

while under alternative $H_1^{(2)}$ it is

$$f_1(\boldsymbol{V}) = \prod_{j=1}^{N}\prod_{i=1}^{M} f_n(v_{ij} - \theta s_i). \tag{21b}$$

Hence the log-likelihood-ratio test for $H_0^{(2)}$ versus $H_1^{(2)}$ is

$$t_{opt} = \ln \Lambda(\boldsymbol{V}) = \sum_{j=1}^{N}\sum_{i=1}^{M} g_i(v_{ij}) \begin{cases} > T_3 \Rightarrow H_1^{(2)} \\ < T_3 \Rightarrow H_0^{(2)} \end{cases} \tag{22}$$

[2] As pointed out in the Introduction, in weak-signal situations, a large number N of samples may be needed to achieve satisfactory system performance. Thus the concept of asymptotic relative efficiency in which the number of samples N approaches infinity is an appropriate measure of performance for such systems.

[3] Details of this calculation are given in [3] however, a similar calculation partially based on work done by Rudnick [4] appears in Helstrom [5].

[4] A proof of this fact was given by Helstrom [5] based on the prior work of Rudnick [4]. An alternative proof using the calculus of variations appears in [3].

where the time-varying nonlinearity $g_i(x)$ is defined as

$$g_i(x) \triangleq \ln [f_n(x - \theta s_i)/f_n(x)]. \tag{23}$$

This test has the structure of Fig. 1 with the linear system $h(\cdot)$ shown in that figure being a summer over the duration of the basic signal. Although the nonlinearity $g_i(x)$ of (23) is simply the optimum nonlinearity $g_{opt}(x)$ of (5) with the parameter θ replaced by θs_i, the fact that it is time varying makes detector implementation more complicated.[5]

Use of the locally optimum, rather than the Neyman–Pearson optimum, detector avoids the problem of implementing a time-varying nonlinearity. Applying the locally optimum test of (6) to the pdf's $f_0(V)$ and $f_1(V)$ of (21a) and (21b) gives

$$t_{lo} = \sum_{j=1}^{N} \sum_{i=1}^{M} s_i g_{lo}(v_{ij}) \begin{cases} > T_4 \Rightarrow H_1^{(2)} \\ < T_4 \Rightarrow H_0^{(2)} \end{cases} \tag{24}$$

where $g_{lo}(\cdot)$ has been defined by (8). The locally optimum detector for time-varying signals thus has the structure of Fig. 1, but with a fixed nonlinearity $g_i(x) = g_{lo}(x)$ for all i. The received data from each channel are first passed through $g_{lo}(\cdot)$ and then through a discrete-time linear system with the impulse response

$$h(i) = \begin{cases} s_{M+1-i}, & i = 1,2,\cdots,M \\ 0, & \text{otherwise.} \end{cases} \tag{25}$$

Finally, the filter outputs from all N channels are summed and compared to a threshold. Note that the linear system $h(i)$ is a matched filter for the extraction of s_i from additive white Gaussian noise. Hence, just as for a constant signal, the locally optimum detector for a signal in white non-Gaussian noise consists of the locally optimum nonlinearity followed by the optimum detector structure for the same signal in white Gaussian noise.

B. ARE of the Time-Varying-Signal Nonlinear Detector of Fig. 1 and Relation to the Locally Optimum Detector

The preceding discussion suggests that suboptimum, as well as optimum and locally optimum, detectors for a known time-varying signal in white non-Gaussian noise might use the structure of Fig. 1, which will henceforth be called a *time-varying-signal nonlinear detector* D_{tn}. This section gives the performance of this detector, as measured by asymptotic relative efficiency. Because of the difficulty of implementing time-varying nonlinearities and to simplify results, the nonlinearity in Fig. 1 is assumed time invariant, that is, $g_i(x) = g(x)$ for all i.

An appropriate detector to which the time-varying-signal nonlinear detector may be compared is the *modified linear detector* D_{ml} that results when we place $g(x) = x$ in the detector of Fig. 1. The linear filter in D_{ml} is denoted by $\hat{h}(\cdot)$.

The ARE of the time-varying-signal nonlinear detector with respect to the modified linear detector, denoted by $ARE_{tn,ml}$, can be calculated in the same manner as for the constant signal by allowing the number of different channels N to approach infinity. Since the calculation is nearly identical to that of (16), no details are given here [3]. The final result is

$$ARE_{tn,ml} = \frac{\sigma_n^2[E\{g'(n_{ij})\}]^2 \quad [\sum_{i=1}^{M} s_i h(M+1-i)]^2 \sum_{i=1}^{M} \hat{h}^2(M+1-i)}{(E\{g^2(n_{ij})\} - [E\{g(n_{ij})\}]^2)[\sum_{i=1}^{M} s_i \hat{h}(M+1-i)]^2 \sum_{i=1}^{M} h^2(M+1-i)}. \tag{26}$$

Note that this last equation factors into the product of two terms. The first term is of the same form as the constant-signal $ARE_{nd,ld}$ of (16), depending only on the nonlinearity $g(\cdot)$ and the noise statistics. The second term depends only on the filters and signal; furthermore, it is equal to 1 if the two filters $h(\cdot)$ and $\hat{h}(\cdot)$ are identical. Thus, for fixed filters $h(\cdot)$ and $\hat{h}(\cdot)$, the nonlinearity $g(\cdot)$ that maximizes $ARE_{tn,ml}$ is the same as that maximizing $ARE_{nd,ld}$, namely the locally optimum nonlinearity $g_{lo}(\cdot)$ [or some linear function of it as in (17)]. Moreover, one can easily show that for a fixed filter $\hat{h}(\cdot)$ in the modified linear detector, the second term in $ARE_{tn,ml}$ is maximized by picking the filter $h(\cdot)$ in the time-varying signal nonlinear detector to be matched, in the sense of (25), to the signal $\{s_i: i = 1,2,\cdots,M\}$. These two results show that, for a fixed modified linear detector, $ARE_{tn,ml}$ is maximized by picking the time-varying nonlinear detector to be the locally optimum detector of (24). As in the constant-signal case, this result should not be surprising.

IV. Examples

In Sections II and III the importance of the Neyman–Pearson optimum nonlinearity $g_{opt}(x)$ and the locally optimum nonlinearity $g_{lo}(x)$ in detectors for constant and time-varying signals was demonstrated. To show the various forms these nonlinearities may take, plots of $g_{opt}(x)$ and $g_{lo}(x)$ are given for various members of three classes of symmetric unimodal noise pdf's. These three classes are generalizations of the Gaussian, Cauchy, and beta distributions. Also because the maximum value of the constant-signal $ARE_{nd,ld}$ is equal to the expression ρ of (19) and because the maximum value of the corresponding time-varying-signal quantity $ARE_{tn,ml}$ is proportional to ρ, plots of ρ as a function of the parameters in these generalized distributions are given.

A. Generalized Gaussian Noise

This class has a symmetric unimodal density obtained by generalizing the Gaussian density [8] to obtain a variable rate of exponential decay and is given by

$$f_n(x) = [c\eta(\sigma_n,c)/2\Gamma(1/c)] \exp\{-[\eta(\sigma_n,c)|x|]^c\} \tag{27a}$$

where for convenience we have defined

$$\eta(\sigma,c) \triangleq \sigma^{-1}[\Gamma(3/c)/\Gamma(1/c)]^{1/2} \tag{27b}$$

[5] Alternatively, as in Algazi and Lerner [6] or Rappaport and Kurz [7], one can pass both the received signal and the received signal from which θs_i has been subtracted through the nonlinearity $\ln [f_n(\cdot)]$ and thus avoid a time-varying nonlinearity.

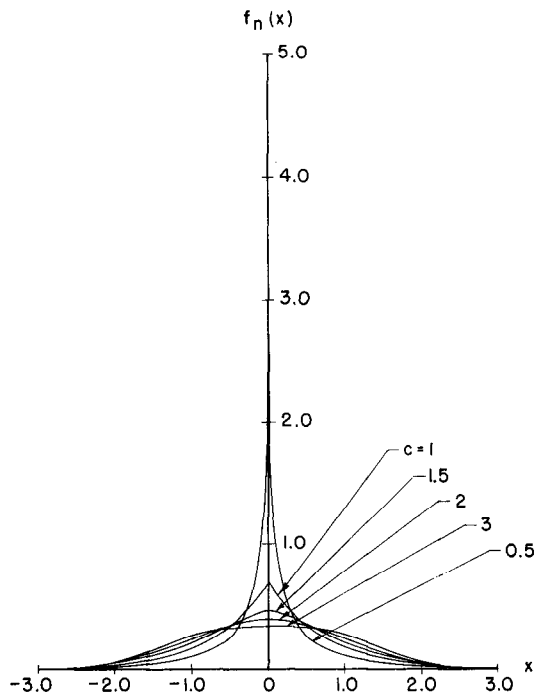

Fig. 3. Generalized Gaussian pdf's ($\sigma_n^2 = 1$).

where c is a positive parameter controlling the rate of decay, $\Gamma(\cdot)$ is the gamma function, and σ_n^2 is the noise variance. Note that for $c = 2$ this density reduces to the Gaussian density, whereas for $c = 1$ it becomes the Laplace density. Furthermore, according to Algazi and Lerner [6], densities representative of certain atmospheric impulse noises can be obtained by picking $0.1 < c < 0.6$. The density of (27) is illustrated in Fig. 3 for values of $\sigma_n^2 = 1.0$ and $c = 0.5$, 1.0, 1.5, 2.0, and 3.0.

Substituting the generalized Gaussian pdf of (27) into (5) for $g_{opt}(x)$ gives

$$g_{opt}(x) = [\eta(\sigma_n,c)]^c(|x|^c - |x - \theta|^c) \tag{28}$$

while substituting (27) into (8) gives[6]

$$g_{lo}(x) = c[\eta(\sigma_n,c)]^c|x|^{(c-1)} \operatorname{sgn}(x). \tag{29}$$

Normalized plots of these two nonlinearities are given in Figs. 4 and 5 for values of $c = 0.5$, 1.0, 1.5, 2.0, and 3.0 and a value of $\theta = 0.5$. Note that as predicted by (10), the nonlinearities $g_{opt}(x)$ and $g_{lo}(x)$ corresponding to the same value of c are quite similar qualitatively. Also note that $g_{opt}(x)$ and $g_{lo}(x)$ satisfy (13) and (14). For $c = 2$, the noise is Gaussian, and both nonlinearities become linear, as expected. For $c = 1$, the noise has the Laplace distribution, and the locally optimum nonlinearity is a hard limiter, which corresponds to the known result [9] that the sign detector is locally optimum for Laplace noise. Also it is clear that the case $c = 1$ is a dividing line between two quite different types of behavior of $g_{opt}(x)$ and $g_{lo}(x)$ for large $|x|$; for rates of decay of $f_n(x)$ slower than exp $(-\alpha|x|)$ both

[6] sgn $(\cdot)$ is the signum function,

$$\operatorname{sgn}(x) = \begin{cases} +1; & x \geq 0 \\ -1; & x < 0. \end{cases}$$

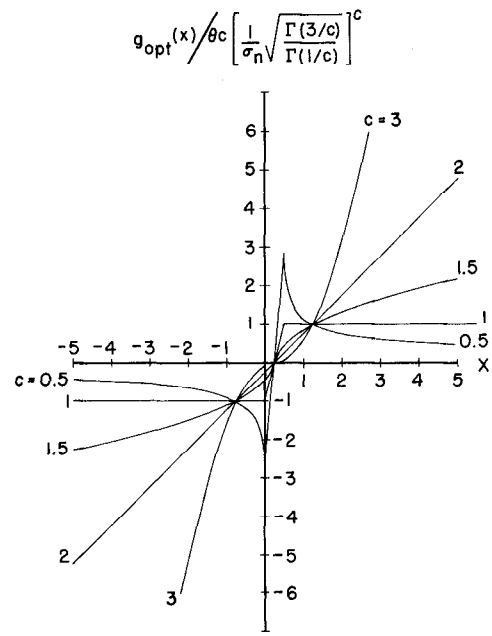

Fig. 4. Normalized Neyman–Pearson optimum nonlinearities for generalized Gaussian noise ($\theta = 0.5$).

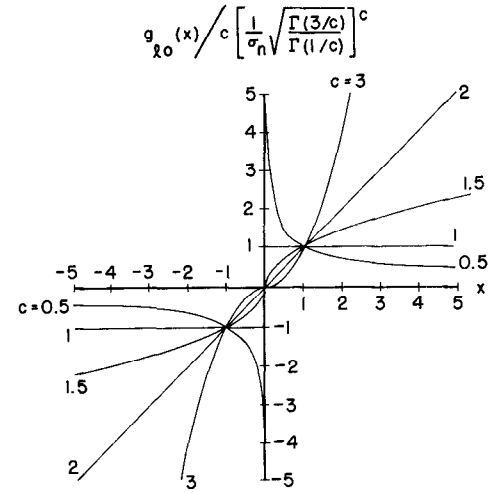

Fig. 5. Normalized locally optimum nonlinearities for generalized Gaussian noise.

nonlinearities approach zero for large $|x|$, while for more rapid decays they approach infinity [see also (9)].

Substituting the density of (27) into the expression for ρ of (19) gives

$$\rho = c^2\Gamma(3/c)\Gamma(2 - 1/c)[\Gamma(1/c)]^{-2}. \tag{30}$$

From this expression it thus follows that the condition (18) to assure a finite ρ is simply that $c > \frac{1}{2}$. Hence for all values of $c > \frac{1}{2}$, (30) gives the maximum ARE obtainable. This equation is plotted as a function of c in Fig. 6. Note that ρ achieves its minimum possible value of 1.0 only for the Gaussian noise case of $c = 2$ when the locally optimum nonlinear filter is the linear filter $g(x) = cx$, and the linear detector is being compared to itself.

To demonstrate the loss in performance resulting from the use of a suboptimum detector, the ARE of the linear detector with respect to the symmetrized sign detector,

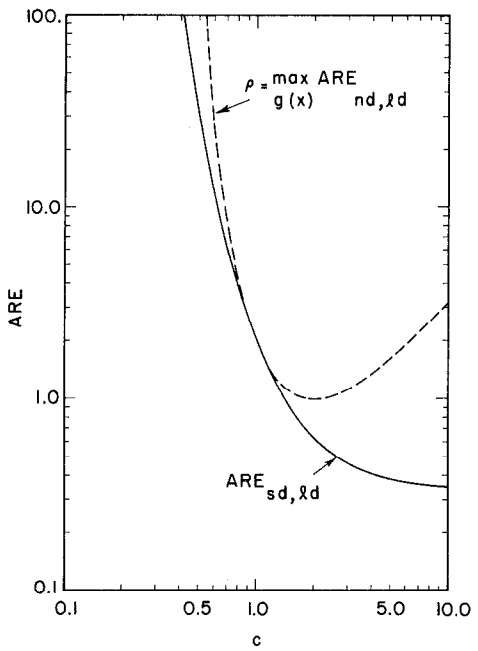

Fig. 6. ρ and $ARE_{sd,ld}$ for generalized Gaussian noise as a function of parameter c.

denoted by $ARE_{sd,ld}$, is also given in this figure. The symmetrized sign detector is obtained by picking as the nonlinearity $g(x)$ in the constant-signal nonlinear detector a hard limiter, i.e.,

$$g(x) = \begin{cases} -c, & x < 0 \\ +c, & x > 0 \end{cases} \tag{31a}$$

where c is any positive constant. Since the derivative of this nonlinearity is

$$g'(x) = 2c\,\delta(x) \tag{31b}$$

where $\delta(\cdot)$ is the Dirac delta function, we get upon substituting (31a) and (31b) into (16) the well-known result for a symmetric unimodal noise pdf

$$ARE_{sd,ld} = 4\sigma_n^2 f_n^2(0) \tag{32}$$

or for the generalized Gaussian density of (27)

$$ARE_{sd,ld} = c^2\Gamma(3/c)[\Gamma(1/c)]^{-3} \tag{33}$$

a result obtained previously [8]. From Fig. 6 we see that ρ and $ARE_{sd,ld}$ have the common value of 2 at $c = 1$; for all other c, the quantity ρ is larger than $ARE_{sd,ld}$, dramatically so for c near $\frac{1}{2}$ or $c \gg 1$. (The coincidence at $c = 1$ is to be expected since the optimum nonlinear detector for $c = 1$ (Laplace noise) is the sign detector.)

B. Generalized Cauchy Noise

It was desired to find a useful class of noise distributions with algebraic rather than exponential decay of $f_n(x)$ for large x and that would approach the generalized Gaussian as some parameter in the distribution approaches infinity, much as the Student's t distribution can be made to approach Gaussian [10]. The resulting distribution will be called generalized Cauchy and takes the form[7]

$$f_n(x) = [c\eta(\sigma,c)/2\Gamma(1/c)][v^{-1/c}\Gamma(v + 1/c)/\Gamma(v)] \cdot \{1 + [\eta(\sigma,c)|x|]^c/v\}^{-(v+1/c)} \tag{34}$$

where c and v are positive parameters. Note that for $c = 2$ and $v = \frac{1}{2}$ we have the Cauchy density.[8] It is shown in [3] that as the parameter v in the distribution of (34) approaches infinity, the resulting distribution approaches the generalized Gaussian distribution of (27). The parameter σ^2 in (34) approaches the variance of the generalized Gaussian distribution as v approaches infinity (see [12]); however, for finite v, the variance of the generalized Cauchy distribution is not σ^2 but rather, as also shown in [3],

$$\sigma_n^2 = \text{var}\,(x) = \sigma^2[v^{2/c}\Gamma(v - 2/c)/\Gamma(v)]. \tag{35}$$

Unlike the generalized Gaussian density, which always has a variance, the preceding variance of the generalized Cauchy density will be finite only if $cv > 2$. To illustrate the density of (34), a set of curves is given in Fig. 7 for $\sigma^2 = 1.0$, $v = 10$, and $c = 0.5$, 1.0, 1.5, 2.0, and 3.0.

Evidence that the generalized Cauchy density (34) is a reasonable one to consider in communication problems is provided by the densities proposed by Mertz [13] and Hall [14] for the amplitude distribution of impulse noise. Mertz assumed that the pdf of the noise amplitude is given by

$$f_{|n|}(x) = vh^v(x + h)^{-(v+1)}, \qquad x \geq 0 \tag{36}$$

where h is a "small" constant and v ranges from just over 2 to about 5. A symmetric unimodal pdf whose amplitude has this pdf is

$$f_n(x) = (1/2)vh^v(h + |x|)^{-(v+1)} \tag{37}$$

but this equation is precisely the pdf of (34) with $c = 1$ and $\sigma^2 = 2h^2/v^2$.

Analogous to (36), the probability density of the amplitude of noise having the generalized Cauchy density of (34) can be shown easily to be, for $x \geq 0$,

$$f_{|n|}(x) = [c\eta(\sigma,c)/\Gamma(1/c)][v^{-1/c}\Gamma(v + 1/c)/\Gamma(v)] \cdot \{1 + [\eta(\sigma,c)x]^c/v\}^{-(v+1/c)}. \tag{38}$$

This equation serves to generalize the Mertz hyperbolic noise amplitude density of (36).

Hall [14] proposed a somewhat different model from that of Mertz and showed that it agrees well with the measured statistics of atmospheric impulse noise. The model assumes that the noise process $n(t)$ has the form

$$n(t) = a(t)z(t) \tag{39}$$

where $z(t)$ is zero-mean Gaussian with variance σ_1^2 and $a(t)$ is a process slowly varying compared to $z(t)$ and

[7] The special case of (34) with $c = 2$ is called the t distribution [11] with $2v$ degrees of freedom, location parameter zero, and precision $1/\sigma$.

[8] The Cauchy noise density itself has been used in several previous papers, such as [7], to represent severe noise despite its pathological nature, i.e., infinite variance.

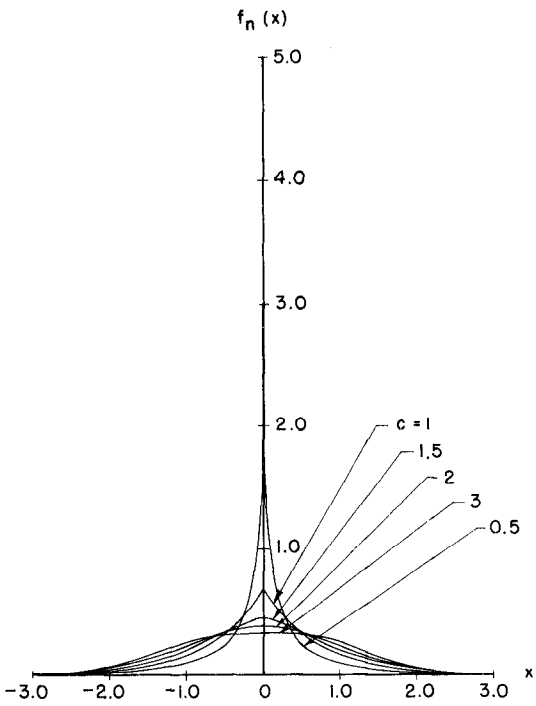

Fig. 7. Generalized Cauchy pdf's ($\sigma^2 = 1$, $v = 10$).

independent of $z(t)$. At any fixed time t_0, the random variable $b \triangleq 1/a(t_0)$ is assumed to have the "two-sided" chi distribution

$$f_b(b) = (m/2)^{m/2}\sigma^{-m}[\Gamma(m/2)]^{-1}|b|^{m-1} \exp[-mb^2/2\sigma^2]. \tag{40}$$

From (39) and (40) it then follows [14] that the first-order pdf of $n \triangleq n(t_0)$ is

$$f_n(x) = \Gamma(\theta/2)\{\Gamma[(\theta - 1)/2]\}^{-1}\gamma^{(\theta-1)}\pi^{-1/2}[\gamma^2 + x^2]^{-\theta/2} \tag{41}$$

where $\gamma \triangleq m^{1/2}\sigma_1/\sigma$ and $\theta \triangleq m + 1 > 1$. This density is the special case of (34) where $c = 2$, $v = (\theta - 1)/2$, and $\sigma^2 = \gamma^2/(\theta - 1)$.

Substituting the density of (34) into (5) gives

$$g_{opt}(x) = v + \frac{1}{c}\ln\frac{1 + [\eta(\sigma,c)|x|]^c/v}{1 + [\eta(\sigma,c)|x - \theta|]^c/v} \tag{42}$$

while substituting this density into (8) gives

$$g_{lo}(x) = \frac{(c + 1/v)[\eta(\sigma,c)]^c|x|^{(c-1)}\operatorname{sgn}(x)}{1 + [\eta(\sigma,c)|x|]^c/v}. \tag{43}$$

By comparing the generalized Cauchy locally optimum nonlinearity of (43) with the corresponding nonlinearity for generalized Gaussian noise (29), we find, as expected, that for a fixed value of x, as $v \to \infty$, the nonlinearity of (43) approaches that of (29). However, on *keeping v fixed* in (43) and letting $|x| \to \infty$, one has

$$\lim_{|x|\to\infty} g_{lo}(x) = 0. \tag{44}$$

Thus, whatever the finite positive values of parameters c and v in the generalized Cauchy density, the corresponding locally optimum (and Neyman–Pearson optimum) nonlinearity approaches zero as $|x|$ approaches infinity. To show this difference in behavior for the generalized Cauchy distribution as compared to the generalized Gaussian, curves are given in Figs. 8 and 9, respectively, for the normalized optimum and locally optimum nonlinearities when $\sigma^2 = 1.0$, $\theta = 0.5$, $v = 10.0$, and c takes on the values of 0.5, 1.0, 1.5, 2.0, and 3.0 as were used in Figs. 4 and 5. From these curves, it is apparent that the behavior for small $|x|$ is quite similar to that of the generalized Gaussian density, while the behavior for large $|x|$ is quite different.

It is shown in [3] that substituting the generalized Cauchy

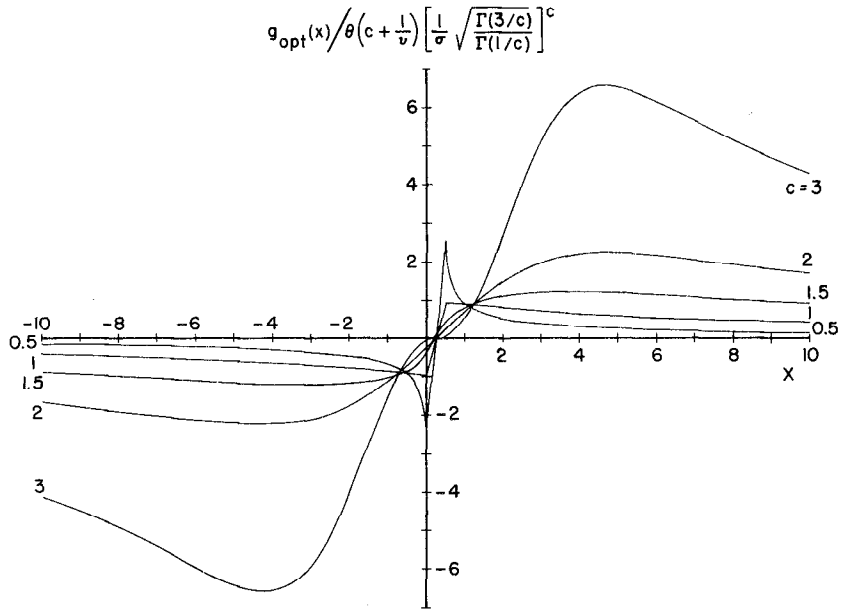

Fig. 8. Normalized Neyman–Pearson optimum nonlinearities for generalized Cauchy noise ($\sigma^2 = 1$, $\theta = 0.5$, $v = 10$).

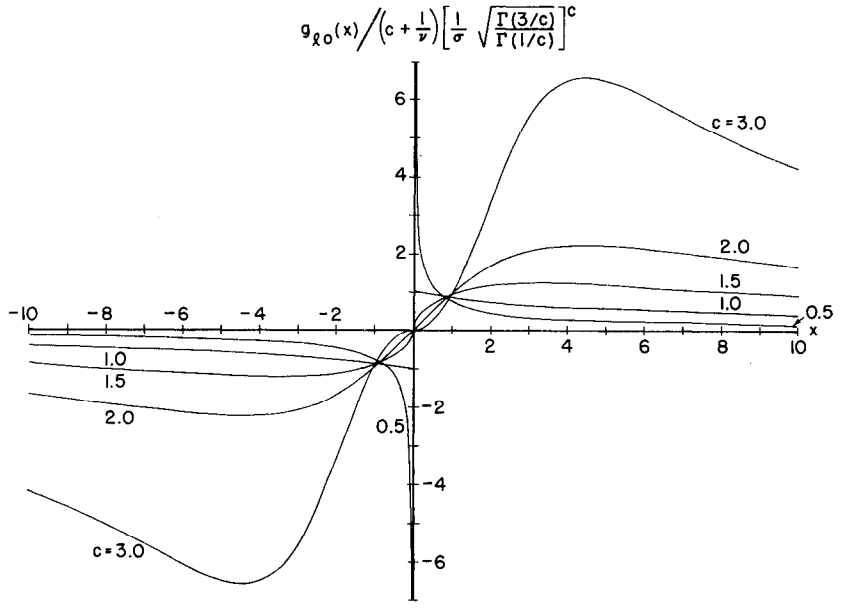

Fig. 9. Normalized locally optimum nonlinearities for generalized Cauchy noise ($\sigma^2 = 1$, $\nu = 10$).

density of (34) into (19) gives

$$\rho = (c\nu + 1)^2 \cdot \frac{\Gamma(3/c)\Gamma(2 - 1/c)\Gamma(\nu - 2/c)\Gamma(\nu + 1/c)\Gamma(\nu + 2/c)}{\Gamma^2(1/c)\Gamma^2(\nu)\Gamma(\nu + 2 + 1/c)} \tag{45}$$

subject to the conditions that $c\nu > 2$ and that $c > \frac{1}{2}$. Note that this second condition is also required for the ρ of generalized Gaussian noise to be finite. Curves of ρ as a function of c, computed from (45), are given in Fig. 10 for values of $\nu = 1$, 3, 5, and 20. Also included in this figure for comparison purposes is the curve for $\nu = \infty$ (generalized Gaussian noise) obtained from (30). The general appearance of the curves for finite ν (generalized Cauchy noise) is much like that for infinite ν (generalized Gaussian noise), except for the $\nu = 1$ curve, which becomes infinite at $c = 2$.

C. Generalized Beta Noise

As with the Cauchy density, a symmetric unimodal beta-type density was desired in order to investigate the forms of the nonlinearities $g_{\text{opt}}(x)$ and $g_{\text{lo}}(x)$ and the performance, as measured by ρ, to be expected for noise pdf's having nonzero values only over a finite interval. It was again decided to make this density approach the generalized Gaussian density of (27) as one of the parameters in the density approaches infinity. The generalized beta density chosen has the form

$$f_n(x) = [c\eta(\sigma,c)/2\Gamma(1/c)] \cdot [\nu^{-1/c}\Gamma(\nu + 1 + 2/c)/\Gamma(\nu + 1 + 1/c)] \cdot \{1 - [\eta(\sigma,c)|x|]^c/\nu\}^{(\nu+1/c)} \tag{46}$$

for $|x| \leq \nu^{1/c}/\eta(\sigma,c)$, where c and ν are positive parameters.

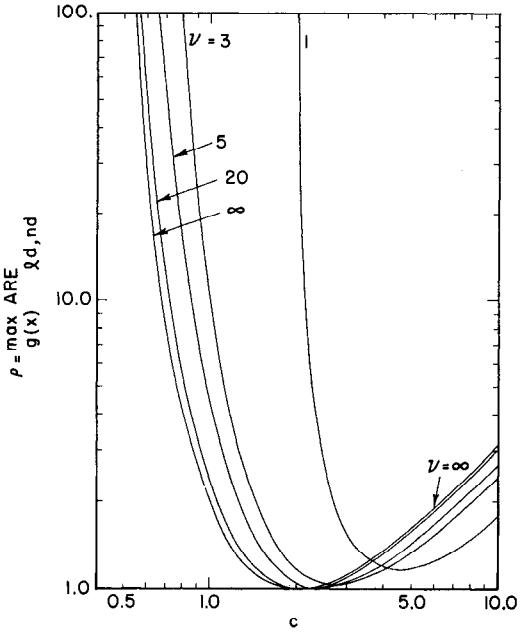

Fig. 10. ρ as a function of parameter c in the generalized Cauchy density.

The density $f_n(x)$ is zero elsewhere. Note that the support of this density must increase with increasing ν. In [3] it is shown that as the parameter ν in the distribution of (46) approaches infinity, the resulting distribution approaches generalized Gaussian. The variance of the density of (46) is also calculated in [3] as

$$\sigma_n^2 = \sigma^2[\nu^{2/c}\Gamma(\nu + 1 + 2/c)/\Gamma(\nu + 1 + 4/c)]. \tag{47}$$

Unlike the variance of generalized Cauchy noise, this variance is finite for all positive c and ν. However, as for generalized Cauchy noise, as $\nu \to \infty$, $\sigma_n^2 \to \sigma^2$. Fig. 11 gives plots of the density of (46) for $\sigma^2 = 1.0$, $\nu = 10.0$, and $c = 0.5$, 1.0, 1.5, 2.0, and 3.0.

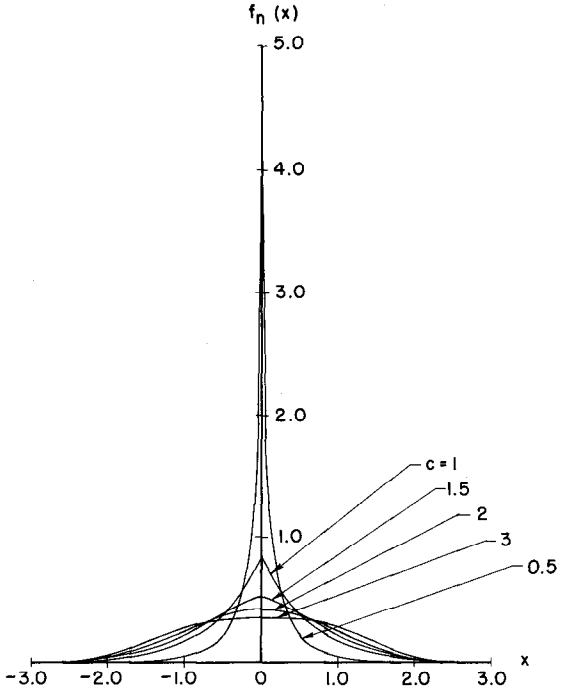

Fig. 11. Generalized beta pdf's ($\sigma^2 = 1$, $v = 10$).

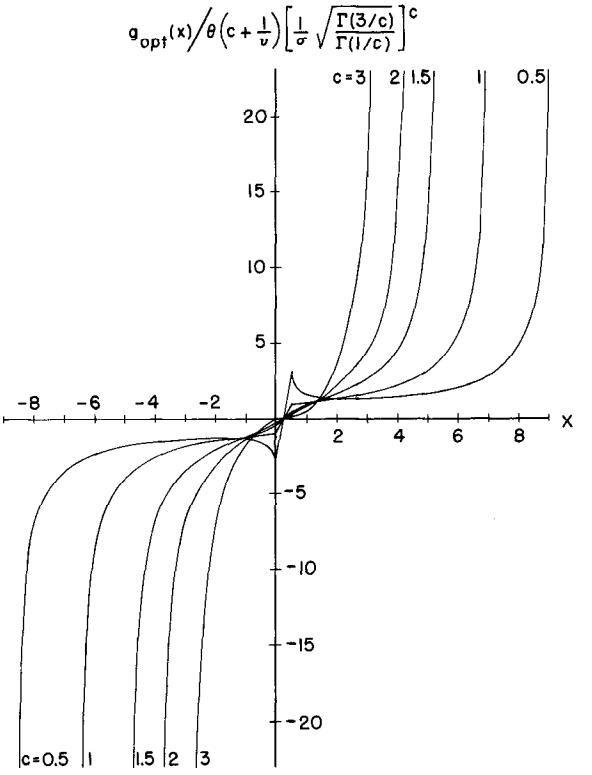

Fig. 12. Normalized Neyman–Pearson optimum nonlinearities for generalized beta noise ($\sigma^2 = 1$, $\theta = 0.5$, $v = 10$).

Substituting (46) into (5) gives

$$g_{opt}(x) = \begin{cases} -\infty, & \dfrac{-v^{1/c}}{\eta(\sigma,c)} \le x \le \dfrac{-v^{1/c}}{\eta(\sigma,c)} + \theta \\ \left(v + \dfrac{1}{c}\right) \ln \dfrac{1 - [\eta(\sigma,c)|x - \theta|]^c/v}{1 - [\eta(\sigma,c)|x|]^c/v}, & \\ & \dfrac{-v^{1/c}}{\eta(\sigma,c)} + \theta < x \le \dfrac{v^{1/c}}{\eta(\sigma,c)} \\ +\infty, & \dfrac{v^{1/c}}{\eta(\sigma,c)} < x \le \dfrac{v^{1/c}}{\eta(\sigma,c)} + \theta \\ 0, & \text{elsewhere.} \end{cases} \quad (48)$$

Note particularly the ranges of x wherein $g_{opt}(x)$ becomes infinite. These regions correspond to values of x for which the signal is either certain to be absent or certain to be present. The nonlinearity $g_{opt}(x)$ for the hypothesis-testing problem $H_0^{(1)}$ versus $H_1^{(1)}$ or $H_0^{(2)}$ versus $H_1^{(2)}$ will obviously always have this property of becoming infinite near the ends of each interval containing the support of any density having finite support.

Substituting (46) into (8) gives, for $|x| \le v^{1/c}/\eta(\sigma,c)$,

$$g_{lo}(x) = \frac{(c + 1/v)[\eta(\sigma,c)]^c |x|^{(c-1)} \operatorname{sgn}(x)}{1 - [\eta(\sigma,c)|x|]^c/v} \quad (49)$$

and zero elsewhere. Again for fixed x, as $v \to \infty$, this nonlinearity approaches that for generalized Gaussian noise [(29)]. Furthermore, it has the value $+\infty$ at $x = v^{1/c}/\eta(\sigma,c)$ and the value $-\infty$ at $x = -v^{1/c}/\eta(\sigma,c)$, which correspond to the regions of infinite value of the optimum nonlinearity of (48).

Figs. 12 and 13 are plots of the optimum and locally optimum nonlinearities, respectively, for generalized beta noise with values of $v = 10$, $\sigma^2 = 1$, $\theta = 0.5$, and $c = 0.5$, 1.0, 1.5, 2.0, and 3.0. Note the similarity for small $|x|$ to the corresponding plots for generalized Gaussian noise and for generalized Cauchy noise. However, for larger $|x|$ nearer the endpoints $\pm v^{1/c}/\eta(\sigma,c)$, both of the generalized beta nonlinearities clearly increase very rapidly in absolute value and thus have very different appearances from the nonlinearities previously considered.

It is shown in [3] that substituting the generalized beta density of (46) into (19) for ρ gives

$$\rho = (cv + 1)^2 \cdot \frac{\Gamma(3/c)\Gamma(2 - 1/c)\Gamma(v - 1 + 1/c)\Gamma^2(v + 1 + 2/c)}{\Gamma^2(1/c)\Gamma(v + 1)\Gamma(v + 1 + 1/c)\Gamma(v + 1 + 4/c)}. \quad (50)$$

The conditions on c and v for the validity of this expression are $c > \frac{1}{2}$ and $v + 1/c > 1$. Curves of ρ as a function of c, computed from (50), are given in Fig. 14 for values of $v = 0.5$, 1.0, 1.3, 2.0, 3.0, 5.0, and 20.0. For comparison purposes, the $v = \infty$ (generalized Gaussian) curve obtained from (30) is also plotted. Again the curves for finite v are very similar to that for infinite v, except for the $v = 0.5$ curve, which becomes infinite at $c = 2$.

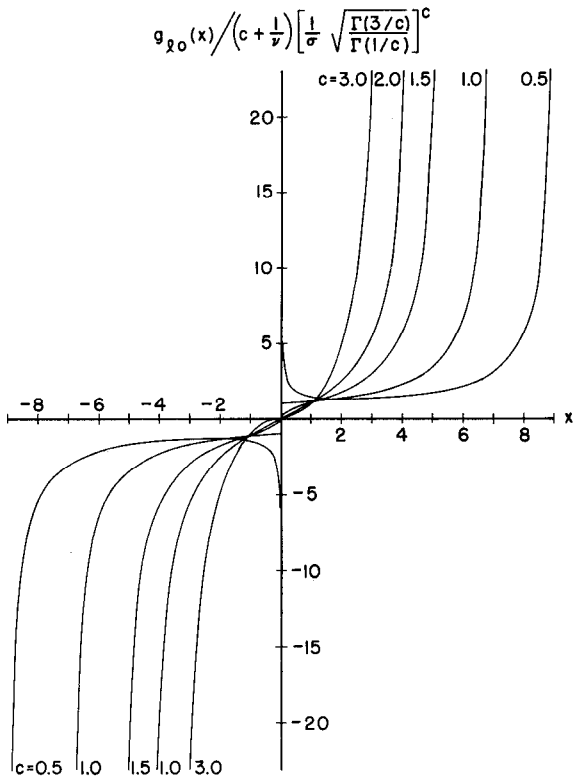

Fig. 13. Normalized locally optimum nonlinearities for generalized beta noise ($\sigma^2 = 1$, $\nu = 10$).

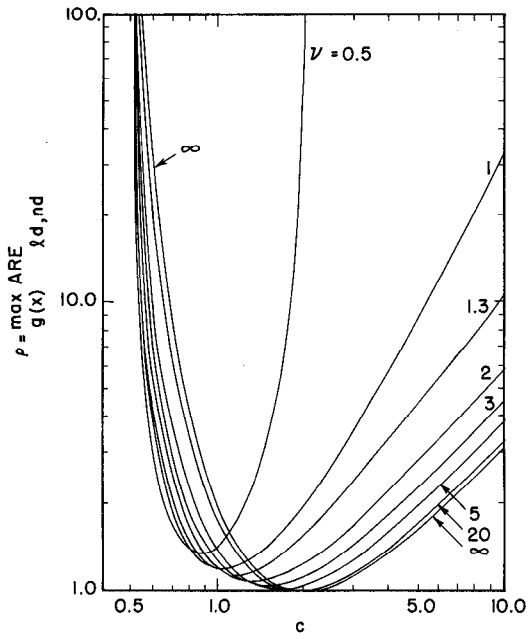

Fig. 14. ρ as a function of parameter c in the generalized beta density.

V. Concluding Comments

In summary, the optimum and locally optimum nonlinearities and resulting maximum AREs have been given for three general classes of probability densities that include as special cases many of the noise pdf's frequently assumed in detection theory. From the examples it is clear that the form of the nonlinearity depends in surprisingly critical ways on the exact noise density. This strong dependence leads to the little-studied question of how much performance is degraded by small errors in the assumed noise density.

Several comments should be made on the applicability to real-world situations of the model used here for the received data. First, we have not considered the effect of a restricted receiver bandwidth. With only a limited bandwidth available, the minimum possible sampling rate of the received analog waveform is in turn fixed. In such a case, the assumption of independent noise samples may be violated, and the structure of an optimum detector could differ considerably from those discussed here.

Second, we have assumed the noise statistics as given at the input to the detector nonlinearity. However, in practice the bandwidths and shapes of the receiver RF and IF filters, which are often partially under the designer's control, can alter considerably the statistics of the non-Gaussian noise at this point. The effect of this additional set of parameters on system performance in non-Gaussian noise has been considered for linear receivers by Engel [15] and for somewhat more general receivers by Bello and Esposito [16].

References

[1] T. S. Ferguson, *Mathematical Statistics: A Decision Theoretic Approach*. New York: Academic Press, 1967.
[2] J. Capon, "On the asymptotic efficiency of locally optimum detectors," *IRE Trans. Inform. Theory*, vol. IT-7, pp. 67–71, Apr. 1961.
[3] J. H. Miller, "Detection of signals in non-Gaussian noise," Ph.D. dissertation, Dep. Elec. Eng., Princeton Univ., Princeton, N.J. (in preparation).
[4] P. Rudnick, "A signal-to-noise property of binary decisions," *Nature*, vol. 193, pp. 604–605, Feb. 10, 1962.
[5] C. W. Helstrom, "Quantum detection theory, *Inform. Contr.*, vol. 10, pp. 254–291, Mar. 1967.
[6] V. R. Algazi and R. M. Lerner, "Binary detection in white non-Gaussian noise," M.I.T. Lincoln Lab., Lexington, Mass., Tech. Rep. DS-2138.
[7] S. S. Rappaport and L. Kurz, "An optimal nonlinear detector for digital data transmission through non-Gaussian channels," *IEEE Trans. Commun. Technol.*, vol. COM-14, pp. 266–274, June 1966.
[8] M. Kanefsky and J. B. Thomas, "On polarity detection schemes with non-Gaussian inputs," *J. Franklin Inst.*, vol. 280, pp. 120–138, 1965.
[9] W. Hoeffding and J. M. Rosenblatt, "The efficiency of tests," *Ann. Math. Statist.*, vol. 26, pp. 52–63, 1955.
[10] M. G. Kendall and A. M. Stuart, *The Advanced Theory of Statistics*, vol. 1: *Distribution Theory*, 2nd ed. New York: Hafner, 1963, pp. 114–115, 376.
[11] M. H. DeGroot, *Optimal Statistical Decisions*. New York: McGraw-Hill, 1970, p. 42.
[12] M. Abramowitz and I. A. Stegun, *Handbook of Mathematical Functions With Formulas, Graphs, and Mathematical Tables* (Applied Mathematics Series 55). Washington, D.C.: NBS, 1965, p. 257, eq. 6.1.46.
[13] P. Mertz, "Model of impulsive noise for data transmission," *IRE Trans. Commun. Syst.*, vol. CS-9, pp. 130–137, June 1961.
[14] H. M. Hall, "A new model for 'impulsive' phenomena: Application to atmospheric-noise communication channels," Stanford Electron. Lab., Stanford Univ., Stanford Calif., Tech. Rep. 3412-8 and 7050-7, Apr. 1966.
[15] J. S. Engel, "Digital transmission in the presence of impulsive noise," *Bell Syst. Tech. J.*, vol. 44, pp. 1699–1743, Oct. 1965.
[16] P. A. Bello and R. Esposito, "A new method for calculating probabilities of errors due to impulsive noise," *IEEE Trans. Commun. Technol.*, vol. COM-17, pp. 368–379, June 1969.